Inorg. Chem. **2005**, *44*, 8011–8022

Syntheses, Structures, and Magnetic Properties of Unusual Nonlinear Polynuclear Copper(II) Complexes Containing Derivatives of 1,2,4-Triazole and Pivalate Ligands

Jian-Hao Zhou,[†] Ru-Mei Cheng,[†] You Song,[†] Yi-Zhi Li,[†] Zhi Yu,[†] Xue-Tai Chen,*[,†,‡] Zi-Ling Xue,[§] and Xiao-Zeng You[†]

Coordination Chemistry Institute, State Key Laboratory of Coordination Chemistry, Nanjing University, Nanjing 210093, People's Republic of China, State Key Laboratory of Structural Chemistry, Fujian Institute of Research on the Structure of Matter, Fuzhou 350002, People's Republic of China, and Department of Chemistry, The University of Tennessee, Knoxville, Tennessee 37996-1600

Received March 31, 2005

Novel polynuclear Cu(II) complexes containing derivatives of 1,2,4-trizaole and pivalate ligands, $[Cu_3(\mu_3\text{-}OH)(\mu\text{-adetrz})_2(piv)_5(H_2O)]\cdot 6.5H_2O$ (**1**) (adetrz = 4-amino-3,5-diethyl-1,2,4-triazole, piv = pivalate), $[Cu_4(\mu_3\text{-}OH)_2(\mu\text{-atrz})_2(\mu\text{-piv})_4(piv)_2]\cdot 2MeOH\cdot H_2O$ (**2**) (atrz = 4-amino-1,2,4-triazole), $[Cu_4(\mu_3\text{-}OH)_2(\mu\text{-tbtrz})_2(\mu\text{-piv})_2(piv)_4]\cdot 4H_2O$ (**3**) (tbtrz = 4-*tert*-butyl-1,2,4-trizaole), and $[Cu_4(\mu_3\text{-}O)_2(\mu\text{-admtrz})_4(admtrz)_2(\mu\text{-piv})_2(piv)_2]\cdot 2[Cu_2(\mu\text{-}H_2O)(\mu\text{-admtrz})(piv)_4]\cdot 13H_2O$ [**4** = **4a**·2(**4b**)·$13H_2O$; admtrz = 4-amino-3,5-dimethyl-1,2,4-triazole], have been prepared and structurally characterized. **1** is an asymmetrical triangular complex containing a $[Cu_3(\mu_3\text{-}OH)]$ core with two Cu---Cu edges spanned by bridging adetrz ligands. **2**, **3**, and **4a** are novel tetranuclear compounds containing a $[Cu_4(\mu_3\text{-}O)_2]$ or $[Cu_4(\mu_3\text{-}OH)_2]$ core with Cu---Cu edges spanned by bridging 1,2,4-triazole or pivalate ligands. **4b** is a dinuclear compound with one admtrz and one water bridge, and it is the first dinuclear Cu(II) triazole complex with one bridging water molecule. **1** is one of few reported triangular Cu(II) complexes with derivatives of 1,2,4-triazole, while **2**, **3**, and **4a** are the first group of the nonlinear tetranuclear Cu(II) compounds with derivatives of 1,2,4-triazole. Variable-temperature magnetic susceptibility studies on the powder samples of **1**–**3** reveal the overall antiferromagnetic coupling between Cu^{II} ions with J values of –55.6 to –12.8 cm^{-1} (**1**), –216.4 to 0 cm^{-1} (**2**), and –259.8 to 4.8 cm^{-1} (**3**).

Introduction

Polynuclear transition metal complexes with derivatives of 1,2,4-triazole have been of growing research interest in recent decades due to their unique magnetic properties.[1] The main research aim in this field is to reveal the underlying magneto-structural correlations[2] and to design novel molecular magnetic materials.[3] The derivatives of 1,2,4-triazole can adopt the monodentate terminal or didentate *N*,*N*′-bridging coordination mode, which makes them easily link two adjacent metal ions to yield dinuclear, linear trinuclear, or linear polymeric metal compounds with double or triple triazole bridges.[1] Considerable progress has been made to reveal the magneto-structural correlation in dinuclear Cu(II) compounds with derivatives of 1,2,4-triazole.[2] In addition, the derivatives of 1,2,4-triazole are useful linkers in the spin-cross Fe(II) molecular systems,[3] which have potential applications in molecular switches and molecular de-

* To whom correspondence should be addressed. E-mail: xtchen@netra.nju.edu.cn.
[†] Nanjing University.
[‡] Fujian Institute of Research on the Structure of Matter.
[§] The University of Tennessee.

(1) (a) Haasnoot, J. G. *Coord. Chem. Rev.* **2000**, *200*, 131−185. (b) Klingele, M. H.; Brooker, S. *Coord. Chem. Rev.* **2003**, *241*, 119−132. (c) Beckmann, U.; Brooker, S. *Coord. Chem. Rev.* **2003**, *245*, 17−29.

(2) (a) Ferrer, S.; van Koningsbruggen, P. J.; Haasnoot, J. G.; Reedijk, J.; Kooijman, H.; Spek, A. L.; Lezama, L.; Arif, A. M.; Miller, J. S. *J. Chem. Soc., Dalton Trans*. **1999**, 4269−4276. (b) Slangen, P. M.; van Koningsbruggen, P. J.; Goubitz, K.; Haasnoot, J. G.; Reedijk, J. *Inorg. Chem.* **1994**, *33*, 1121−1126. (c) Slangen, P. M.; van Koningsbruggen, P. J.; Haasnoot, J. G.; Jansen, J.; Gorter, S.; Reedijk, J.; Kooijman, H.; Smeets, W. J. J.; Spek, A. L. *Inorg. Chim. Acta* **1993**, *212*, 289−301. (d) Koomen-van Oudenniel, W. M. E.; de Graaff, R. A. G.; Haasnoot, J. G.; Prins, R.; Reedijk, J. *Inorg. Chem*. **1989**, *28*, 1128−1133. (e) Klingele, M. H.; Boyd, P. D. W.; Moubaraki, B.; Murray, K. S.; Brooker, S. *Eur. J. Inorg. Chem.* **2005**, 910−918.

10.1021/ic050475x CCC: $30.25 © 2005 American Chemical Society
Published on Web 09/23/2005

vices.[4] Hence, Fe(II)-triazole compounds have been prepared to find the room-temperature spin-cross molecular materials.[3] Many Cu(II) triazole compounds have been reported, including dinuclear,[2,5] linear trinuclear,[6] one-dimensional chain,[7] two-dimensional network,[8] trinuclear triangular,[9] and hexanuclear ring[10] complexes with the triazole bridge. However, few nonlinear polynuclear Cu(II) compounds with derivatives of 1,2,4-triazole are known in the literature.[9]

On the other hand, carboxylates have been proven to be a group of remarkable ligands exhibiting versatile coordination modes in the build-up of polynulear metal compounds, which play a key role in the studies of molecular magnetic materials.[11,12,14] Recently, many polynuclear metal carboxylates, especially manganese carboxylate compounds, have been found to exhibit single molecular magnetism (SMM).[11] Pivalate, a carboxylate ligand with a sterically demanding substituent and varied bridging capability, has recently attracted particular attention because metal pivalates often exhibit molecular structures different from those of normal metal acetates.[12] Therefore, many polynuclear metal pivalates have been studied to establish reliable synthetic routes to oligomeric structures in polynuclear coordination chemistry. Moreover, the good solubility of metal pivalates in organic solvents is favorable for crystallization of the products.

Scheme 1. The Derivatives of 1,2,4-Triazole Used in the Current Work

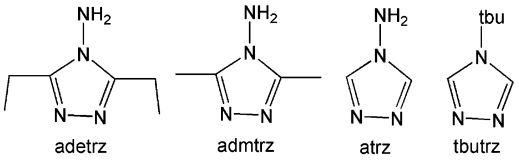

The reported polynuclear metal triazole compounds often contain anions, for example, Cl^-, OH^-, N_3^-, SCN^-,[1] etc., which are an essential part of the coordination polyhedra.[1a] However, the carboxylate ligand used as a co-ligand with derivatives of 1,2,4-triazole in polynuclear metal compounds was rarely studied. Only one dinuclear copper compound containing 1,2,4-triazole and carboxylate ligands, that is, $[Cu_2(CH_3CO_2)_4(admtrz)_2]$ (admtrz = 4-amino-3,5-dimethyl-1,2,4-triazole), has been reported up until now.[13] Many studies have indicated that the use of two kinds of bridging organic ligands leads to polynuclear metal compounds with higher nuclearity and novel structures.[14] Thus, the use of triazole and pivalate ligands might be expected to yield novel polynuclear metal compounds.

In this paper, we report the synthesis and structures of four polynuclear Cu(II) compounds containing derivatives of 1,2,4-triazole and pivalate ligands, $[Cu_3(\mu_3\text{-}OH)(\mu\text{-adetrz})_2(piv)_5(H_2O)]\cdot 6.5H_2O$ (**1**) (adetrz = 4-amino-3,5-diethyl-1,2,4-triazole, piv = pivalate), $[Cu_4(\mu_3\text{-}OH)_2(\mu\text{-atrz})_2(\mu\text{-piv})_4(piv)_2]\cdot 2MeOH\cdot H_2O$ (**2**) (atrz = 4-amino-1,2,4-triazole), $[Cu_4(\mu_3\text{-}OH)_2(\mu\text{-tbtrz})_2(\mu\text{-piv})_2(piv)_4]\cdot 4H_2O$ (**3**) (tbtrz = 4-*tert*-butyl-1,2,4-trizaole), and $[Cu_4(\mu_3\text{-}O)_2(\mu\text{-admtrz})_4(admtrz)_2(\mu\text{-piv})_2(piv)_2]\cdot 2[Cu_2(\mu\text{-}H_2O)(\mu\text{-admtrz})(piv)_4]\cdot 13H_2O$ [**4** = **4a**·2(**4b**)·$13H_2O$; admtrz = 4-amino-3,5-dimethyl-1,2,4-triazole]. The structures of the triazole ligands are depicted in Scheme 1. The magnetic properties of **1**−**3** are also described.

Experimental Section

General. $[Cu(Me_3CCOO)_2]_2$,[15] 4-amino-1,2,4-triazole (atrz),[16] 4-amino-3,5-diethyl-1,2,4-triazole (adetrz),[16] 4-amino-3,5-dimethyl-

(3) (a) Haasnoot, J. G. In *Magnetism: A supramolecular Function*; Kahn, O., Ed.; Kluwer Academic Publishers: The Netherlands, 1996; pp 299−321. (b) Garcia, Y.; Moscovici, J.; Michalowicz, A.; Ksenofontov, V.; Levchenko, G.; Bravic, G.; Chasseau, D.; Gütlich, P. *Chem.-Eur. J.* **2002**, *8*, 4992−5000. (c) Roubeau, O.; Gomez, J. M. A.; Balskus, E.; Kolnaar, J. J. A.; Haasnoot, J. G.; Reedijk, J. *New J. Chem.* **2001**, *25*, 144−150. (d) Kolnaar, J. J. A.; de Heer, M. I.; Kooijman, H.; Spek, A. L.; Schmitt, G.; Ksenofontov, V.; Gütlich, P.; Haasnoot, J. G.; Reedijk, J. *Eur. J. Inorg. Chem.* **1999**, 881−886. (e) Klingele, M. H.; Moubaraki, B.; Cashion, J. D.; Murray, K. S.; Brooker, S. *Chem. Commun.* **2005**, 987−989.

(4) (a) Kahn, O.; Martinez, C. J. *Science* **1998**, *279*, 44−48. (b) Zarembowitch, J.; Kahn, O. *New J. Chem.* **1991**, *15*, 181−190. (c) Kahn, O.; Krober, J.; Jay, C. *Adv. Mater.* **1992**, *4*, 718−728.

(5) Castillo, O.; Garcia-Couceiro, U.; Luque, A.; Garcia-Teran, J. P.; Roman, P. *Acta Crystallogr.* **2004**, *E60*, m9−m11.

(6) (a) Vreugdenhil, W.; Haasnoot, J. G.; Reedijk, J.; Wood, J. S. *Inorg. Chim. Acta* **1990**, *167*, 109−113. (b) Liu, J.-C.; Fu, D.-G.; Zhuang, J.-Z.; Duan, C.-Y.; You, X.-Z. *J. Chem. Soc., Dalton Trans.* **1999**, 2337−2342. (c) Tang, J.-K.; Wang H.-M.; Cheng, P.; Liu, X.; Liao, D.-Z.; Jiang, Z.-H.; Yan, S.-P. *Polyhedron* **2001**, *20*, 675−680. (d) van Koningsbruggen, P. J.; van Hal, J. W.; de Graaff, R. A. G.; Haasnoot, J. G.; Reedijk, J. *J. Chem. Soc., Dalton Trans.* **1993**, 2163−2167. (e) Liu, J.-C.; Song, Y.; Yu, Z.; Zhuang, J.-Z.; Huang, X.-Y.; You, X.-Z. *Polyhedron* **1999**, *18*, 1491−1494. (f) Shakirova, O. G.; Virovets, A. V.; Naumov, D. Y.; Shvedenkov, Y. G.; Elokhina, V. N.; Lavrenova, L. G. *Inorg. Chem. Commun.* **2002**, *5*, 690−693.

(7) (a) Drabent, K.; Ciunik, Z. *Chem. Commun.* **2001**, 1254−1255. (b) Garcia, Y.; van Koningsbruggen, P. J.; Bravic, G.; Chasseau, D.; Kahn, O. *Eur. J. Inorg. Chem.* **2003**, 356−362. (c) Garcia, Y.; van Koningsbruggen, P. J.; Bravic, G.; Guionneau, P.; Chasseau, D.; Cascarano, G. L.; Moscovici, J.; Lambert, K.; Michalowicz, A.; Kahn, O. *Inorg. Chem.* **1997**, *36*, 6357−6365. (d) Jarvis, J. A. *Acta Crystallogr.* **1962**, *15*, 964−966. (e) Klingele, M. H.; Brooker, S. *Inorg. Chim. Acta* **2004**, *357*, 3413−3417.

(8) Engelfriet, D. W.; den Brinker, W.; Verschoor, G. C.; Gorter, S. *Acta Crystallogr., Sect. B* **1979**, *35*, 2922−2927.

(9) (a) Liu, J.-C.; Guo, G.-C.; Huang, J.-S.; You, X.-Z. *Inorg. Chem.* **2003**, *42*, 235−243. (b) Ferrer, S.; Lloret, F.; Bertomeu, I.; Alzuet, G.; Borrás, J.; García-Granda, S.; Liu-González, M.; Haasnoot, J. G. *Inorg. Chem.* **2002**, *41*, 5821−5830. (c) Ferrer, S.; Haasnoot, J. G.; Reedijk, J.; Müller, E.; Cingi, M. B.; Lanfranchi, M.; Lanfredi, A. M. M.; Ribas, J. *Inorg. Chem.* **2000**, *39*, 1859−1867.

(10) Liu, J.-C.; Zhuang, J.-Z.; You, X.-Z.; Huang, X.-Y. *Chem. Lett.* **1999**, *7*, 651−652.

(11) (a) Aromí, G.; Aubin, S. M. J.; Bolcar, M. A.; Christou, G.; Eppley, H. J.; Folting, K.; Hendrickson, D. N.; Huffman, J. C.; Squire, R. C.; Tsai, H.-L.; Wang, S.; Wemple, M. W. *Polyhedron* **1998**, *17*, 3005−3020. (b) Foguet-Albiol, D.; O'Brien, T. A.; Wernsdorfer, W.; Moulton, B.; Zaworotko, M. J.; Abboud, K. A.; Christou, G. *Angew. Chem., Int. Ed.* **2005**, *44*, 897−901. (c) Brechin, E. K.; Sañudo, E. C.; Wernsdorfer, W.; Boskovic, C.; Hendrickson, D. N.; Yamaguchi, A.; Ishimoto, H.; Concolino, T. E.; Rheingold, A. L.; Christou, G. *Inorg. Chem.* **2005**, *44*, 502−511. (d) Murugesu, M.; Clérac, R.; Anson, C. E.; Powell, A. K. *Inorg. Chem.* **2004**, *43*, 7269−7271. (e) Murugesu, M.; King, P.; Clérac, R.; Anson, C. E.; Powell, A. K. *Chem. Commun.* **2004**, 740−741.

(12) (a) Christian, P.; Rajaraman, G.; Harrison, A.; Helliwell, M.; McDouall, J. J. W.; Raftery, J.; Winpenny, R. E. P. *Dalton Trans.* **2004**, 2550−2555. (b) Murrie, M.; Parsons, S.; Winpenny, R. E. P. *J. Chem. Soc., Dalton Trans.* **1998**, 1423−1424. (c) Mikuriya, M.; Azuma, H.; Nukada, R.; Handa, M. *Chem. Lett.* **1999**, 57−58. (d) Aromí, G.; Batsanov, A. S.; Christian, P.; Helliwell, M.; Parkin, A.; Parsons, S.; Smith, A. A.; Timco, G. A.; Winpenny, R. E. P. *Chem.-Eur. J.* **2003**, *9*, 5142−5161. (e) Eremenko, I. L.; Nefedov, S. E.; Sidorov, A. A.; Moiseev, I. L. *Russ. Chem. Bull.* **1999**, *48*, 405−416. (f) Eremenko, I. L.; Nefedov, S. E.; Sidorov, A. A.; Golubnichaya, M. A.; Danilov, P. V.; Ikorskii, V. N.; Shvedenkov, Y. G.; Novotortsev, V. M.; Moiseev, I. I. *Inorg. Chem.* **1999**, *38*, 3764−3773.

(13) Liu, J.-C.; Zhuang, J.-Z.; You, X.-Z. *Chin. J. Inorg. Chem.* **2000**, *16*, 27−30.

(14) (a) Winpenny, R. E. P. *Adv. Inorg. Chem.* **2001**, *52*, 1−111. (b) Winpenny, R. E. P. *J. Chem. Soc., Dalton Trans.* **2002**, 1−10. (c) Blake, A. J. Grant, C. M.; Gregory, C. I.; Parsons, S.; Rawson, J. M.; Reed, D.; Winpenny, R. E. P. *J. Chem. Soc., Dalton Trans.* **1995**, 163−175.

1,2,4-triazole (admtrz),[16] and 4-*tert*-butyl-1,2,4-triazole (tbtrz)[17] were prepared by the literature methods. Potassium pivalate (Kpiv) was synthesized in water by treatment of Me_3CCOOH with KOH in a 1:1 molar ratio. All other reagents were purchased from commercial sources and used without further purification. Elemental analyses (C, H, and N) were carried out on a Perkin-Elmer 240C analytical instrument. IR spectra were recorded on a VECTOR 22 Bruker spectrophotometer with KBr pellets in the 4000−400 cm^{-1} region. DC magnetic susceptibilities of the powder samples of **1**−**3** were carried out with a Quantum Design MPMS-XL SQUID magnetometer in the 1.8−300 K range. The applied magnetic field was 2 kG, and the data were corrected for diamagnetism using Pascal's constants and the temperature-independent paramagnetism estimated at 60×10^{-6} emu/mol per Cu^{II} ion. The X-band EPR spectra were recorded on a Bruker EMX-10/12 spectrometer on polycrystalline samples or frozen solution at 110 K.

Preparation of $[Cu_3(\mu_3\text{-OH})(\mu\text{-adetrz})_2(piv)_5(H_2O)]\cdot 6.5H_2O$ (1). To a 10 mL ethanol solution of $[Cu(piv)_2]_2$ (0.2 g, 0.38 mmol) was added adetrz (0.11 g, 0.76 mmol) with stirring. The resulting solution was stirred at room temperature for 4 h and then filtered. Blue crystals were obtained by slow evaporation of the resulting solution (0.15 g, yield 53.5%, based on $[Cu(piv)_2]_2$). Anal. Calcd for $C_{37}H_{85}Cu_3N_8O_{18.5}$(%): C, 39.37; H, 7.59; N, 9.93. Found: C, 39.66; H, 7.26; N, 10.08. IR (KBr pellet, cm^{-1}): 3299(w), 3173(w), 2975(s), 2959(s), 2871(w), 1593(vs), 1568(vs), 1483(s), 1459(w), 1410(s), 1360(s), 1224(s), 1060(w), 892(w), 791(w), 618(w).

Preparation of $[Cu_4(\mu_3\text{-OH})_2(atrz)_2(piv)_6]\cdot 2MeOH\cdot H_2O$ (2). To a 10 mL ethanol solution of $[Cu(piv)_2]_2$ (0.3 g, 0.56 mmol) was added atrz (0.094 g, 1.12 mmol) with stirring. The solution was stirred at room temperature for 4 h and then filtered. The resulting blue precipitate was dissolved in MeOH and then filtered off. The filtrate was left at room temperature, and blue crystals were precipitated in a few days (0.16 g, yield 50%, based on $[Cu(piv)_2]_2$). Anal. Calcd for $C_{36}H_{74}Cu_4N_8O_{17}$(%): C, 37.76; H, 6.51; N, 9.79. Found: C, 37.52; H, 6.76; N, 9.51. IR (KBr pellet, cm^{-1}): 3443(m), 3161(w), 2960(m), 2930(w), 2870(w), 1640(w), 1588(m), 1552(vs), 1483(s), 1459(w), 1421(s), 1409(s), 1359(s), 1224(m), 1070(m), 893(w), 797(w), 625(m).

Preparation of $[Cu_4(\mu_3\text{-OH})_2(\mu\text{-tbtrz})_2(\mu\text{-piv})_2(piv)_4]\cdot 4H_2O$ (3). To a 10 mL ethanol solution of $[Cu(piv)_2]_2$ (0.20 g, 0.38 mmol) was added tbutrz (0.094 g, 0.76 mmol) with stirring. The resulting solution was stirred at room temperature for 4 h and then filtered. Blue crystals were obtained by slow evaporation of the resulting solution (0.11 g, yield 47.6%, based on $[Cu(piv)_2]_2$). Anal. Calcd for $C_{42}H_{86}Cu_4N_6O_{18}$(%): C, 41.44; H, 7.12; N, 6.90. Found: C, 41.57; H, 7.39; N, 6.65. IR (KBr pellet, cm^{-1}): 3426(m), 3173(w), 2958(s), 2929(w), 2868(w), 1605(s), 1562(vs), 1482(s), 1460(w), 1420(s), 1398(s), 1357(s), 1222(s), 1076(m), 1028(w), 882(w), 792(w), 658(w), 612(w).

Preparation of $[Cu_4(\mu_3\text{-O})_2(\mu\text{-admtrz})_4(admtrz)_2(\mu\text{-piv})_2(piv)_2]\cdot 2[Cu_2(\mu\text{-}H_2O)(\mu\text{-admtrz})(piv)_4]\cdot 13H_2O$ (4 = 4a·2(4b)·13H$_2$O). To a 10 mL ethanol solution of $Cu(NO_3)_2\cdot 3H_2O$ (0.3 g, 1.24 mmol) were added Kpiv (0.35 g, 2.48 mmol) and admtrz (0.28 g, 2.50 mmol) with stirring. The resulting solution was stirred at room temperature for 4 h and then filtered. The filtrate was evaporated to dryness at room temperature to give a blue residue, which was extracted with acetonitrile and filtered. Blue crystals were obtained by slow evaporation of the resulting solution (0.091 g, yield 20%, based on $Cu(NO_3)_2\cdot 3H_2O$). Anal. Calcd for $C_{92}H_{202}Cu_8N_{32}O_{41}$(%): C, 37.83; H, 6.97; N, 15.34. Found: C, 38.02; H, 7.23; N, 15.61. IR (KBr pellet, cm^{-1}): 3329(s), 2957(m), 2929(w), 2870(w), 1604(s), 1547(s), 1482(m), 1459(w), 1411(m), 1360(m), 1267(w), 1221(m), 1098(w), 1046(w), 1011(w), 965(w), 885(w), 797(w), 779(w), 738(w), 664(w), 615(w), 535(w).

X-ray Crystal Structure Determination. Parameters for data collection and refinement of **1**−**4** are summarized in Table 1. Intensities of **1**−**4** were collected on a Bruker SMART-CCD diffractometer with graphite-monochromated Mo Kα ($\lambda = 0.71073$ Å). The structures were solved by direct methods and refined on F^2 using full-matrix least-squares methods with SHELXTL version 6.1.[18] The hydrogen atoms H1a in **1**−**3** and H6a, H6b in **4** were found in a difference Fourier map and not refined; the rest were positioned geometrically and refined in the riding-model approximation. All non-hydrogen atoms in **1**−**4** were refined anisotropically. Disorders were observed for the C atoms of the *tert*-butyl groups in **1** and **3**, and they were refined over two sites with occupancies of 0.519(6), 0.519(6), and 0.519(6) for C13, C14, and C15 in **1**, and 0.061(5) for C19 in **3**, respectively.

Results and Discussion

Synthesis of 1−4. 1−**4** were obtained by the treatment of $[Cu(piv)_2]_2$ with the corresponding triazoles in ethanol at room temperature. The mixture of $[Cu(piv)_2]_2$ and the corresponding derivatives of 1,2,4-triazole in a molar ratio of 1:2 was found to give pure crystalline **1**−**3** with reasonable yields (40−55% based on $[Cu(piv)_2]_2$). However, this route was found to give **4** in a low yield (10%). Excess triazole is required, as otherwise the unreacted precusor $[Cu(piv)_2]_2$ crystallizes from the solution, giving a low yield of the product. Direct self-assembly reactions using $Cu(NO_3)_2\cdot 3H_2O$ were tried as well to prepare **1**−**4**. A reaction of $Cu(NO_3)_2\cdot 3H_2O$, Kpiv, and triazole in the molar ratio of 1:2:2 gave **1**−**4** in 20−30% yield, but the reaction mixture of the correct stoichiometric molar ratio did not yield pure **1**−**4**. These studies showed that the use of the preformed dinuclear $[Cu(piv)_2]_2$ was not necessary for the preparation of **1**−**4**. We have not optimized the reaction conditions for the self-assembly of **1**−**4**.

Molecular Structures of 1−4. The molecular structures and crystal packing of **1**−**4** are shown in Figures 1−8. The selected bond distances and bond angles of **1**−**4** are listed in Tables 2−5.

Structure of $[Cu_3(\mu_3\text{-OH})(\mu\text{-adetrz})_2(piv)_5(H_2O)]\cdot 6.5H_2O$ (1). 1 is a trinuclear complex with a $[Cu_3(\mu_3\text{-OH})]^{5+}$ core (Figure 1), where the μ_3-OH group is 0.605 Å above the Cu_3 plane. Both Cu1---Cu3 and Cu1---Cu2 edges have a bridging adetrz ligand, whereas no bridging ligand spans the Cu2---Cu3 edge. Cu1 shows distorted tetragonal pyramidal coordination with the Addison parameter τ value of 0.33.[19] The basal plane of Cu1 is completed by O1 of the μ_3-OH group [Cu1−O1, 1.9741(19) Å], N5 from one bridging adetrz [Cu1−N5, 2.028(3) Å], and O atoms from two terminal pivalate ligands [Cu1−O8, 1.926(2) Å; Cu1−O10, 1.963(2) Å], respectively. The apical position is occupied by N1

(15) Muto, Y.; Hirashima, N.; Tokii, T.; Kato, M.; Suzuki, I. *Bull. Chem. Soc. Jpn.* **1986**, *59*, 3672−3674.
(16) Herbst, R. M.; Garrison, J. A. *J. Org. Chem.* **1953**, *18*, 872−877.
(17) Groeneveld, L. R.; Le Febre, R. A.; de Graaff, R. A. G.; Haasnoot, J. G.; Vos, G.; Reedijk, J. *Inorg. Chim. Acta* **1985**, *102*, 69−82.
(18) Sheldrick, G. M. *SHELXTL-NT*, version 6.1; Bruker AXS, Inc.: Madison, WI, 2000.
(19) Addison, A. W.; Rao, T. N.; Reedijk, J.; van Rijn, J.; Verschoor, G. C. *J. Chem. Soc., Dalton Trans.* **1984**, 1349−1356.

Table 1. Crystallographic Data for **1**−**4**[a]

	1	**2**	**3**	**4**
empirical formula	$C_{74}H_{170}Cu_6N_{16}O_{37}$	$C_{72}H_{148}Cu_8N_{16}O_{34}$	$C_{42}H_{86}Cu_4N_6O_{18}$	$C_{92}H_{202}Cu_8N_{32}O_{41}$
formula mass	2257.50	2290.38	1217.33	2921.18
T (K)	293(2)	293(2)	293(2)	293(2)
λ (Å)	0.71073	0.71073	0.71073	0.71073
crystal system	monoclinic	monoclinic	triclinic	triclinic
space group	$P2_1/c$	$P2_1/c$	$P\bar{1}$	$P\bar{1}$
a (Å)	13.176(2)	13.942(2)	9.933(5)	14.843(3)
b (Å)	22.736(4)	19.243(2)	13.475(7)	16.772(3)
c (Å)	19.606(3)	11.728(1)	13.758(7)	16.935(3)
α (deg)			110.756(9)	69.443(4)
β (deg)	96.132(3)°	101.708(2)	101.800(9)	89.050(3)
γ (deg)			104.429(9)	65.844(3)
V (Å^3)	5839.8(16)	3081.0(5)	1578.1(13)	3561.6(12)
Z	2	1	1	1
D_c (g/cm^3)	1.284	1.234	1.281	1.362
μ (mm^{-1})	1.149	1.421	1.392	1.252
F(000)	2392	1196	640	1538
crystal size (mm)	0.20 × 0.25 × 0.32	0.15 × 0.25 × 0.30	0.15 × 0.20 × 0.30	0.08 × 0.20 × 0.25
θ range for data collection (deg)	1.79−26.00	1.83−26.00	1.82−26.00	1.83−25.25
ranges of h,k,l	$-16 \le h \le 15$ $-26 \le k \le 28$ $-24 \le l \le 23$	$-17 \le h \le 16$ $-23 \le k \le 18$ $-13 \le l \le 14$	$-12 \le h \le 12$ $-15 \le k \le 16$ $-16 \le l \le 16$	$-17 \le h \le 17$ $-19 \le k \le 20$ $-9 \le l \le 20$
reflections collected/unique	31 017/11 386	16 376/6060	8574/6061	18 278/12 663
R_{int}	0.0338	0.0827	0.0258	0.0217
data/restraints/parameters	11 386/0/651	6060/0/308	6061/0/336	12 663/0/805
GOF on F^2	0.999	1.030	0.983	1.058
a, b in weighting scheme	0.07, 1.88	0.08, 1.88	0.06, 1.22	0.05, 1.85
final R1/wR2 indices [$I > 2\sigma(I)$]	0.0494/0.1163	0.0641/0.1534	0.0541/0.1159	0.0544/0.1086
final R1/wR2 indices (all data)	0.0684/0.1231	0.1244/0.1736	0.0733/0.1202	0.0741/0.1130
largest diff. peak/hole (e Å^{-3})	0.223/−0.430	0.402/−0.985	0.409/−0.794	1.027/−0.651

[a] $R_1 = \sum||F_o| - |F_c||/\sum|F_o|$, $wR_2 = [\sum w(|F_o|^2 - |F_c|^2)/\sum w|F_o|^2]^{1/2}$, GOF $= [\sum[w(F_o^2 - F_c^2)^2]/(n-p)]^{1/2}$, $w = 1/[\sigma^2(F_o^2) + (aP)^2 + bP]$, where $P = (F_o^2 + 2F_c^2)/3$.

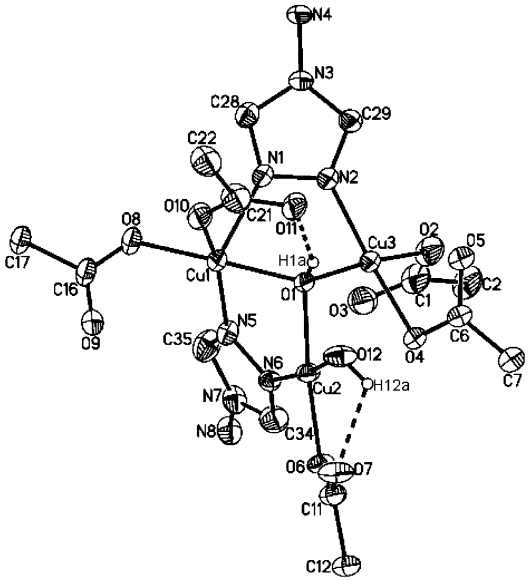

Figure 1. ORTEP drawing (30% probability level) of **1**; all H atoms (except H1a and H12a), lattice water, the ethyl groups in adetrz, and methyl groups in pivalates have been omitted for clarity.

Table 2. Selected Bond Lengths (Å) and Angles (deg) in **1**

Cu(1)−O(8)	1.926(2)	Cu(2)−O(6)	1.954(2)
Cu(1)−O(10)	1.963(2)	Cu(2)−O(1)	1.9607(19)
Cu(1)−O(1)	1.9741(19)	Cu(3)−O(1)	1.967(2)
Cu(1)−N(5)	2.028(3)	Cu(3)−N(2)	1.988(3)
Cu(1)−N(1)	2.260(3)	Cu(3)−O(2)	1.921(3)
Cu(2)−N(6)	2.017(3)	Cu(3)−O(4)	1.976(2)
Cu(2)−O(12)	1.953(2)		
Cu(1)···Cu(3)	3.339(1)	Cu(2)···Cu(3)	3.192(1)
Cu(1)···Cu(2)	3.189(1)		
O(8)−Cu(1)−O(10)	86.68(11)	O(1)-Cu(2)-N(6)	83.65(9)
O(8)−Cu(1)−O(1)	179.00(10)	O(2)−Cu(3)−O(1)	171.84(11)
O(1)−Cu(1)−O(10)	93.42(9)	O(2)−Cu(3)−O(4)	90.15(11)
O(8)−Cu(1)−N(5)	95.95(11)	O(1)−Cu(3)−O(4)	87.35(9)
N(5)−Cu(1)−O(10)	159.24(11)	O(2)−Cu(3)−N(2)	94.80(11)
O(1)−Cu(1)−N(5)	83.61(9)	O(1)−Cu(3)−N(2)	88.84(9)
O(8)−Cu(1)−N(1)	97.10(10)	O(4)−Cu(3)−N(2)	170.36(11)
N(1)−Cu(1)−O(10)	93.85(11)	Cu(2)−O(1)−Cu(3)	108.70(9)
O(1)−Cu(1)−N(1)	83.88(9)	Cu(2)−O(1)−Cu(1)	108.30(9)
N(5)−Cu(1)−N(1)	106.20(11)	Cu(3)−O(1)−Cu(1)	115.83(10)
O(6)−Cu(2)−O(12)	91.88(9)	N(2)−N(1)−Cu(1)	115.53(18)
O(1)−Cu(2)−O(12)	90.92(9)	N(1)−N(2)−Cu(3)	118.18(19)
O(6)−Cu(2)−O(1)	172.47(9)	N(6)−N(5)−Cu(1)	116.90(18)
N(6)−Cu(2)−O(12)	173.62(10)	N(5)−N(6)−Cu(2)	115.59(17)
O(6)−Cu(2)−N(6)	93.91(9)		

from one bridging adetrz [Cu1−N1, 2.260(3) Å]. Both Cu2 and Cu3 are in a nearly square planar configuration. Besides O1 of the μ_3-OH group [Cu2−O1, 1.9607(19) Å; Cu3−O1, 1.967(2) Å], Cu2 is coordinated by N6 from one bridging adetrz [Cu2−N6, 2.017(3) Å], O6 from one terminal pivalate [Cu2−O6, 1.954(2) Å] and one water molecule [Cu2−O12, 1.953(2) Å], respectively, while Cu3 is surrounded by N2 from one bridging adetrz [Cu3−N2, 1.988(3) Å] and O atoms from two terminal pivalate ligands [Cu3−O2, 1.921(3) Å; Cu3−O4, 1.976(2) Å]. The dihedral angle between the coordination plane of Cu2 and the basal plane of Cu1 is 57.07°. The Cu−O−Cu angles have a "one large + two small" isosceles pattern with the large angle Cu1−O1−Cu3 being opposite to Cu2. **1** is best described as an asymmetrically bridged trinuclear triangular Cu(II) complex due to different coordination environments of three copper atoms,

Table 3. Selected Bond Lengths (Å) and Angles (deg) in **2**[a]

Cu(1)−O(2)	1.890(4)	Cu(2)−O(1)	1.901(3)
Cu(1)−O(1)	1.947(3)	Cu(2)−O(5)$^{\#1}$	1.914(3)
Cu(1)−N(3)	1.955(5)	Cu(2)−O(6)	1.932(4)
Cu(1)−O(4)	1.979(4)	Cu(2)−N(1)	2.014(5)
Cu(1)−O(6)$^{\#1}$	2.388(4)	Cu(2)−O(1)$^{\#1}$	2.362(4)
Cu(1)···Cu(2)	3.394(1)	Cu(2)···Cu(2)$^{\#1}$	3.164(1)
Cu(1)···Cu(2)$^{\#1}$	3.131(1)	Cu(1)···Cu(1)$^{\#1}$	5.712(1)
O(2)−Cu(1)−O(1)	170.74(16)	O(1)−Cu(2)−N(1)	85.90(16)
O(2)−Cu(1)−N(3)	91.09(17)	O(5)$^{\#1}$−Cu(2)−N(1)	87.40(16)
O(1)−Cu(1)−N(3)	84.70(17)	O(6)−Cu(2)−N(1)	168.54(17)
O(2)−Cu(1)−O(4)	88.13(15)	O(1)−Cu(2)−O(1)$^{\#1}$	84.79(14)
O(1)−Cu(1)−O(4)	96.86(15)	O(5)$^{\#1}$−Cu(2)−O(1)$^{\#1}$	94.63(14)
N(3)−Cu(1)−O(4)	174.33(17)	O(6)−Cu(2)−O(1)$^{\#1}$	82.19(15)
O(2)−Cu(1)−O(6)$^{\#1}$	106.87(15)	N(1)−Cu(2)−O(1)$^{\#1}$	109.26(14)
O(1)−Cu(1)−O(6)$^{\#1}$	81.21(13)	Cu(2)−O(1)−Cu(1)	123.72(18)
N(3)−Cu(1)−O(6)$^{\#1}$	87.11(16)	Cu(2)−O(1)−Cu(2)$^{\#1}$	95.21(14)
O(4)−Cu(1)−O(6)$^{\#1}$	87.74(14)	Cu(1)−O(1)−Cu(2)$^{\#1}$	92.68(13)
O(1)−Cu(2)−O(5)$^{\#1}$	172.67(14)	Cu(2)−O(6)−Cu(1)$^{\#1}$	92.27(16)
O(1)−Cu(2)−O(6)	94.93(14)	N(1)−N(3)−Cu(1)	125.0(4)
O(5)$^{\#1}$−Cu(2)−O(6)	92.22(14)	N(3)−N(1)−Cu(2)	119.1(3)

[a] Symmetry transformations used to generate equivalent atoms: #1, $-x+1, -y+2, -z+1$.

Table 4. Selected Bond Lengths (Å) and Angles (deg) in **3**[a]

Cu(1)−O(3)	1.925(3)	Cu(2)−O(2)	1.941(3)
Cu(1)−O(1)	1.927(3)	Cu(2)−O(6)	1.949(3)
Cu(1)−O(4)	1.928(3)	Cu(2)−N(1)	1.982(3)
Cu(1)−N(2)$^{\#1}$	1.982(3)	Cu(2)−O(1)	2.302(3)
Cu(2)−O(1)$^{\#1}$	1.923(3)		
Cu(2)···Cu(2)$^{\#1}$	3.101(2)	Cu(1)···Cu(2)	3.103(2)
Cu(1)···Cu(2)$^{\#1}$	3.389(2)	Cu(1)···Cu(1)$^{\#1}$	5.711(2)
O(3)−Cu(1)−O(1)	94.35(11)	O(6)−Cu(2)−N(1)	161.06(13)
O(3)−Cu(1)−O(4)	89.46(12)	O(1)$^{\#1}$−Cu(2)−O(1)	85.99(11)
O(1)−Cu(1)−O(4)	174.90(12)	O(2)−Cu(2)−O(1)	96.12(11)
O(3)−Cu(1)−N(2)$^{\#1}$	177.96(14)	O(6)−Cu(2)−O(1)	89.53(11)
O(1)−Cu(1)−N(2)$^{\#1}$	86.39(13)	N(1)−Cu(2)−O(1)	109.38(12)
O(4)−Cu(1)−N(2)$^{\#1}$	89.91(13)	Cu(2)$^{\#1}$−O(1)−Cu(1)	123.33(13)
O(1)$^{\#1}$−Cu(2)−O(2)	173.90(12)	Cu(2)$^{\#1}$−O(1)−Cu(2)	94.01(11)
O(1)$^{\#1}$−Cu(2)−O(6)	95.82(12)	Cu(1)−O(1)−Cu(2)	94.00(11)
O(2)−Cu(2)−O(6)	89.94(13)	N(2)−N(1)−Cu(2)	120.6(3)
O(1)$^{\#1}$−Cu(2)−N(1)	86.77(13)	N(1)−N(2)−Cu(1)$^{\#1}$	119.7(2)
O(2)−Cu(2)−N(1)	87.13(14)		

[a] Symmetry transformations used to generate equivalent atoms: #1, $-x+2, -y+1, -z+1$.

which is consistent with the magnetic susceptibility measurement (see below). A large number of trinuclear triangular Cu(II) complexes have been reported in the past decades,[20] among which a few complexes with derivatives of the triazole have been studied.[9] Here, **1** is an unprecedented example as an asymmetrically bridged trinuclear triangular Cu(II) complex with the derivative of the triazole. The molecular structure features two intramolecular hydrogen bonds O1−H1a···O11 with an O1·····O11 distance of 2.613(3) Å and O12−H12a···O7 with an O12·····O7 distance of 2.540(3) Å (Figure 1, Table 1S). The molecular packing of **1** viewed down the *a* axis is shown in Figure 2. A two-dimensional layered structure of molecules is formed through five types of intermolecular hydrogen bonds: N4−H4E···O7$^{\#1}$, N4−H4D···O9$^{\#2}$, N8−H8D···O5$^{\#3}$, O13−H13G···O10, and O14−H14H···O13$^{\#4}$ (Table 1S).

Table 5. Selected Bond Lengths (Å) and Angles (deg) in **4**[a]

4a			
Cu(1)−O(1)	1.979(2)	Cu(2)−N(2)	2.230(3)
Cu(1)−O(4)	2.015(3)	Cu(2)−O(1)	1.959(2)
Cu(1)−N(5)	2.017(3)	Cu(2)−O(1)$^{\#1}$	1.989(2)
Cu(1)−N(1)$^{\#1}$	2.041(3)	Cu(2)−O(2)	2.007(2)
Cu(1)−O(3)	2.372(3)	Cu(2)−N(9)	2.008(3)
Cu(1)−N(10)$^{\#1}$	2.450(3)		
Cu(1)···Cu(2)$^{\#1}$	3.2783(8)	Cu(2)···Cu(2)$^{\#1}$	2.9719(9)
Cu(1)···Cu(2)	3.4421(8)	Cu(1)···Cu(1)$^{\#1}$	6.0298(12)
O(1)−Cu(1)−O(4)	92.66(10)	O(2)−Cu(2)−N(9)	89.72(12)
O(1)−Cu(1)−N(5)	173.39(10)	O(1)−Cu(2)−N(2)	91.52(11)
O(4)−Cu(1)−N(5)	90.21(11)	O(1)$^{\#1}$−Cu(2)−N(2)	86.38(10)
O(1)−Cu(1)−N(1)$^{\#1}$	87.14(11)	O(2)−Cu(2)−N(2)	98.66(11)
O(4)−Cu(1)−N(1)$^{\#1}$	177.80(13)	N(9)−Cu(2)−N(2)	96.51(13)
N(5)−Cu(1)−N(1)$^{\#1}$	89.76(12)	O(1)−Cu(2)−Cu(2)$^{\#1}$	41.56(6)
O(1)−Cu(1)−O(3)	88.22(9)	O(1)$^{\#1}$−Cu(2)−Cu(2)$^{\#1}$	40.79(6)
O(4)−Cu(1)−O(3)	91.35(11)	O(2)−Cu(2)−Cu(2)$^{\#1}$	141.35(8)
N(5)−Cu(1)−O(3)	97.66(11)	N(9)−Cu(2)−Cu(2)$^{\#1}$	127.35(10)
N(1)$^{\#1}$−Cu(1)−O(3)	90.83(12)	N(2)−Cu(2)−Cu(2)$^{\#1}$	88.58(9)
O(1)−Cu(1)−N(10)$^{\#1}$	80.79(10)	N(2)−N(1)−Cu(1)$^{\#1}$	115.5(2)
O(4)−Cu(1)−N(10)$^{\#1}$	85.05(11)	N(1)−N(2)−Cu(2)	114.3(2)
N(5)−Cu(1)−N(10)$^{\#1}$	93.54(12)	N(6)−N(5)−Cu(1)	119.6(2)
N(1)$^{\#1}$−Cu(1)−N(10)$^{\#1}$	92.76(12)	N(10)−N(9)−Cu(2)	114.2(2)
O(3)−Cu(1)−N(10)$^{\#1}$	168.25(10)	N(9)−N(10)−Cu(1)$^{\#1}$	111.7(2)
O(1)−Cu(2)−O(1)$^{\#1}$	82.35(9)	N(14)−N(13)−Cu(3)	116.6(2)
O(1)−Cu(2)−O(2)	100.03(10)	N(13)−N(14)−Cu(4)	119.0(2)
O(1)$^{\#1}$−Cu(2)−O(2)	174.33(10)	Cu(2)−O(1)−Cu(1)	121.89(11)
O(1)−Cu(2)−N(9)	166.32(12)	Cu(2)−O(1)−Cu(2)$^{\#1}$	97.65(9)
O(1)$^{\#1}$−Cu(2)−N(9)	87.10(12)	Cu(1)−O(1)−Cu(2)$^{\#1}$	111.42(10)
4b			
Cu(3)−O(6)	1.874(3)	Cu(4)−O(6)	1.973(3)
Cu(3)−O(9)	2.002(3)	Cu(4)−N(14)	1.992(3)
Cu(3)−O(7)	2.003(3)	Cu(4)−O(13)	2.010(3)
Cu(3)−N(13)	2.044(3)	Cu(4)−O(11)	2.011(3)
Cu(3)···Cu(4)	3.2740(9)		
O(6)−Cu(3)−O(9)	94.64(13)	O(6)−Cu(4)−N(14)	85.18(12)
O(6)−Cu(3)−O(7)	170.26(14)	O(6)−Cu(4)−O(13)	170.01(13)
O(9)−Cu(3)−O(7)	84.39(13)	N(14)−Cu(4)−O(13)	93.90(13)
O(6)−Cu(3)−N(13)	88.17(12)	O(6)−Cu(4)−O(11)	90.19(11)
O(9)−Cu(3)−N(13)	176.53(14)	N(14)−Cu(4)−O(11)	170.05(13)
O(7)−Cu(3)−N(13)	93.19(13)	O(13)−Cu(4)−O(11)	92.17(12)
Cu(3)−O(6)−Cu(4)	116.64(14)		

[a] Symmetry transformations used to generate equivalent atoms: #1, $-x+1, -y+1, -z+2$.

Structure of $[Cu_4(\mu_3\text{-}OH)_2(\mu\text{-}atrz)_2(\mu\text{-}piv)_4(piv)_2]\cdot 2MeOH\cdot H_2O$ (2). The structure of **2** consists of a tetranuclear $[Cu_4(\mu_3\text{-}OH)_2]$ core with a center of inversion (Figure 3). The μ_3-OH group is 0.799 Å apart from the Cu_4 plane. Both Cu1 and Cu2 exhibit the tetragonal pyramidal geometry with the τ values[19] of 0.060 and 0.069, which is very close to the value of 0 for an ideal square pyramidal configuration. The dihedral angle between the two basal planes of Cu1 and Cu2 is 13.05°. The two copper atoms Cu1 and Cu2, separated

(20) (a) Casarin, M.; Corvaja, C.; di Nicola, C.; Falcomer, D.; Franco, L.; Monari, M.; Pandolfo, L.; Pettinari, C.; Piccinelli, F.; Tagliatesta, P. *Inorg. Chem.* **2004**, *43*, 5865−5876. (b) Angaridis, P. A.; Baran, P.; Boèa, R.; Cervantes-Lee, F.; Haase, W.; Mezei, G.; Raptis, R. G.; Werner, R. *Inorg.* Chem. **2002**, *41*, 2219−2228. (c) Hulsbergen, F. B.; ten Hoedt, R. W. T.; Verschoor, G. C.; Reedijk, J.; Spek, A. L. *J. Chem. Soc., Dalton Trans.* **1983**, 539−545. (d) Angaroni, M.; Ardizzoia, G. A.; Beringhelli, T.; La Monica, G.; Gatteschi, D.; Masciocchi, N.; Moret, M. J. *J. Chem. Soc., Dalton Trans.* **1990**, 3305−3309. (e) Boèa, R.; Dlháò, L.; Mezei, G.; Ortiz-Pérez, T.; Raptis, R. G.; Telser, J. *Inorg. Chem.* **2003**, *42*, 5801−5803. (f) Costes, J.-P.; Dahan, F.; Laurent, J.-P. *Inorg. Chem.* **1986**, *25*, 413−416. (g) Butcher, R. J.; O'Connor, C. J.; Sinn, E. *Inorg. Chem.* **1981**, *20*, 537−545. (h) Shen, W. Z.; Yi, L.; Cheng, P.; Yan, S. P.; Liao, D. Z.; Jiang, Z. H. *Inorg. Chem. Commun.* **2004**, *7*, 819−822. (i) Liu, X. M.; de Miranda, M. P.; Mclnnes, E. J. L.; Kilner, C. A.; Halcrow, M. A. *Dalton Trans.* **2004**, 59−64. (j) Chaudhuri, P.; Karpenstein, I.; Winter, M.; Butzlaff, C.; Bill, E.; Trautwein, A. X.; Flöke, U.; Haupt, H.-J. *J. Chem. Soc., Chem. Commun.* **1992**, 321−322. (k) Cage, B.; Cotton, F. A.; Dalai, N. S.; Hillard, E. A.; Rakvin, B.; Ramsey, C. M. *J. Am. Chem. Soc.* **2003**, *125*, 5271−5272.

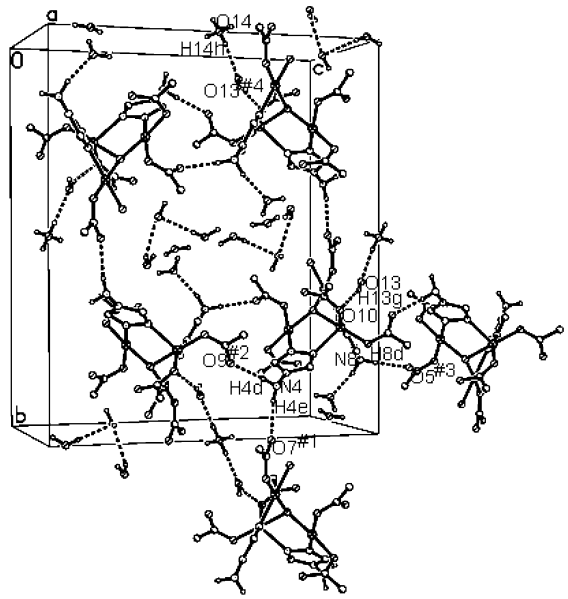

Figure 2. The molecular packing of **1** in the crystal lattice. The ethyl groups in adetrz and methyl groups in pivalates have been omitted for clarity [symmetry code: #1, $-x + 2$, $y + {}^1/_2$, $-z + {}^3/_2$; #2, x, $-y + {}^3/_2$, $z - {}^1/_2$; #3, x, $-y + {}^3/_2$, $z + {}^1/_2$; #4, $-x + 2$, $y - {}^1/_2$, $-z + {}^3/_2$].

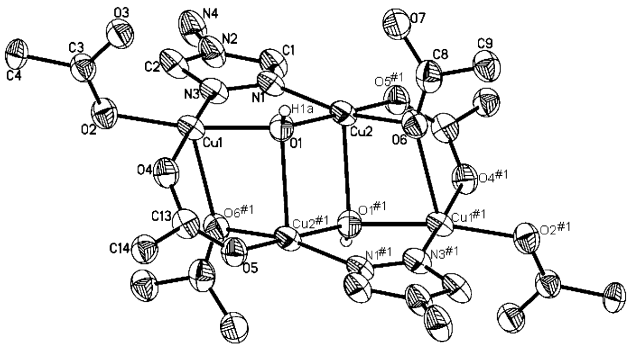

Figure 3. ORTEP drawing (30% probability level) of **2**; all H atoms (except H1a and H1a$^{\#1}$), lattice water, methanol, and methyl groups in pivalates have been omitted for clarity [symmetry code: #1, $1 - x$, $2 - y$, $1 - z$].

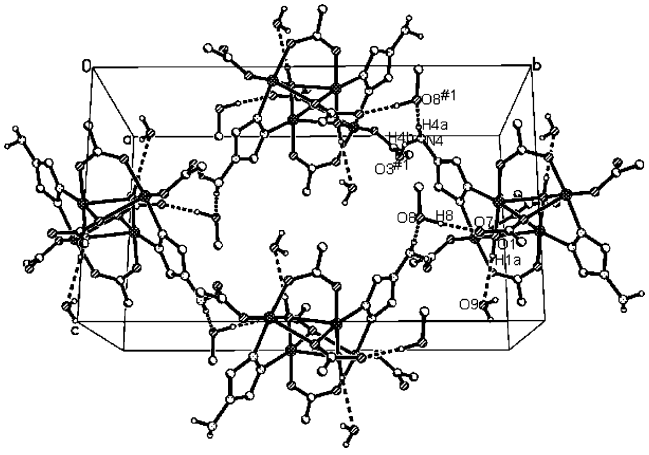

Figure 4. The molecular packing of **2**. Methyl groups in pivalates have been omitted for clarity [symmetry code: #1, x, $-y + {}^3/_2$, $z - {}^1/_2$].

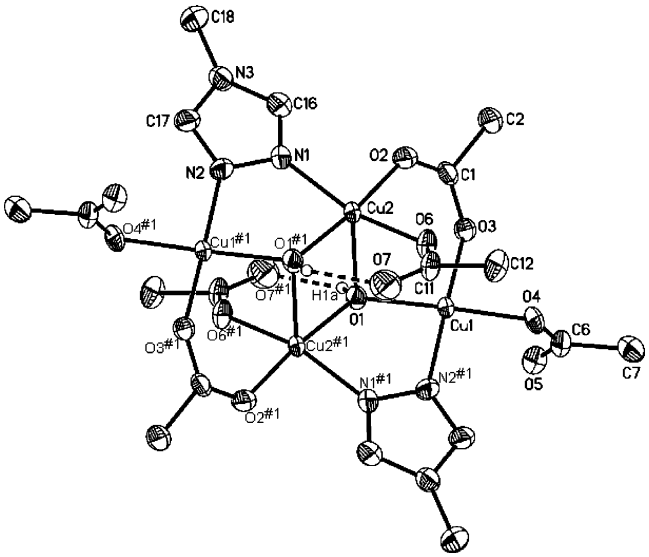

Figure 5. ORTEP drawing (30% probability level) of **3**; all H atoms (except H1a and H1a$^{\#1}$), lattice water, and methyl groups in pivalates and tbtrz have been omitted for clarity [symmetry code: #1, $-x + 2$, $-y + 1$, $-z + 1$].

by 3.394(1) Å, are bridged by one bridging atrz and one μ_3-OH oxygen atom. The structural framework can be viewed as a dimer of the dinuclear unit of Cu1 and Cu2 and its symmetrical equivalence connected by four axially long bonds [Cu1−O6$^{\#1}$, 2.388(4) Å; Cu2−O1$^{\#1}$, 2.362(4) Å] and two 1,3-briding pivalate ligands. The Cu−O−Cu angles, viz., Cu2−O1−Cu1, Cu2−O1−Cu2$^{\#1}$, and Cu1−O1−Cu2$^{\#1}$, are 123.72(18)°, 95.21(14)°, and 92.68(13)°, respectively. It is interesting to observe that the Cu2---Cu1$^{\#1}$ edge is spanned by two pivalate ligands in 1,3 and 1,1 bridging modes, which is a rarely reported phenomenon,[21a,b] although monatomic bridging carboxylates have been known in a few complexes.[21c−g] The crystal packing of **2** is shown in Figure 4. A two-dimensional structure of molecules is assembled through three types of intermolecular hydrogen bonds, N4−H4A···O8$^{\#1}$, N4−H4B···O3$^{\#1}$, and O8−H8···O7 (Table 2S).

Structure of [Cu$_4$(μ_3-OH)$_2$(μ-tbtrz)$_2$(μ-piv)$_2$(piv)$_4$]·4H$_2$O (3). The structure of **3** is similar to that of **2**. **3** is a tetranuclear complex containing a [Cu$_4$(μ_3-OH)$_2$] core with a center of inversion (Figure 5). The μ_3-OH group is 0.801 Å apart from the Cu$_4$ plane. Cu1 is displaced by 0.0101(13) Å from the Cu1−O3−O1−N2$^{\#1}$−O4 mean plane (a), while Cu2 is displaced by 0.1352(13) Å from the Cu2−O2−O6−O1$^{\#1}$−N1 mean plane (b). The dihedral angle between (a) and (b) is 14.29°. The Cu−O−Cu angles [123.33(13)°, 94.01(11)°, 94.00(11)°] are closely comparable to those in **2**. Cu1 is in square planar configuration with four surrounding donor atoms, O1 of the triply bridging hydroxyl group [Cu1−O1, 1.927(3) Å], N2$^{\#1}$ from one bridging tbtrz ligand [Cu1−N2$^{\#1}$, 1.982(3) Å], O4 from one terminal pivalate ligand [Cu1−O4, 1.928(3) Å], and O3 from one 1,3-bridging

(21) (a) Christou, G.; Perlepes, S. P.; Libby, E.; Folting, K.; Huffman, J. C.; Webb, R. J.; Hendrickson, D. N. *Inorg. Chem.* **1990**, *29*, 3657−3666. (b) Chiari, B.; Tarantelli, T.; Zanazzi, P. F. *Inorg. Chem.* **1985**, *24*, 4615−4619. (c) Butcher, R. J.; Overman, J. W.; Sinn, E. *J. Am. Chem. Soc.* **1980**, *102*, 3276−3278. (d) Greenaway, A. M.; O'Connor, C. J.; Wvermna, J. W.; Sinn, E. *Inorg. Chem.* **1981**, *20*, 1508−1513. (e) Chiri, B.; Hatefield, W. E.; Piovesana, O.; Tarantelli, T.; Haar, L. W.; Zanazzi, P. F. *Inorg. Chem.* **1983**, *22*, 1468−1473. (f) Costes, J. P.; Dahan, F.; Laurent, J. P. *Inorg. Chem.* **1985**, *24*, 1018−1022. (g) Chiari, B.; Helms, J. H.; Piovesana, O.; Tarantelli, T.; Zanazzi, P. F. *Inorg. Chem.* **1986**, *25*, 870−874.

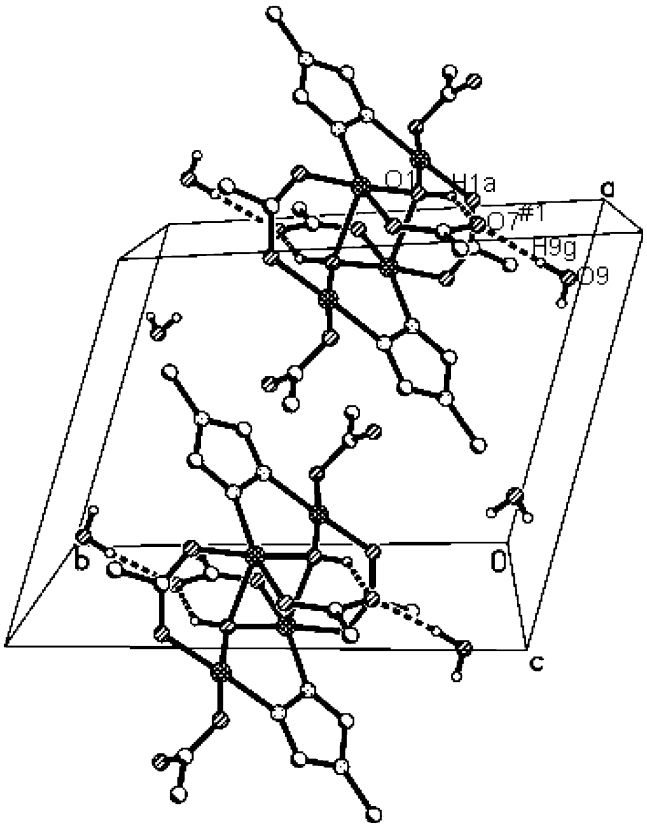

Figure 6. Molecular packing of **3**. Methyl groups in pivalates and tbtrz have been omitted for clarity [symmetry code: #1, $-x+2, -y+1, -z+1$].

pivalate ligand [Cu1−O3, 1.925(3) Å]. Cu2 is in a tetragonal pyramidal configuration ($\tau = 0.21$)[19] with four relatively short bonds in the basal plane [Cu2−N1, 1.982(3) Å; Cu2−O2, 1.941(3) Å; Cu2−O1$^{\#1}$, 1.927(3) Å; and Cu2−O2, 1.949(3) Å] and an axially long bond [Cu2−O1, 2.302(3) Å]. The Cu1---Cu2 and Cu1---Cu2$^{\#1}$ edge distances are 3.103(2) and 3.389(2) Å, respectively. There are two intramolecular hydrogen bonds: O1−H1a···O7$^{\#1}$ with the O1---O7$^{\#1}$ distance of 2.702(5) Å and its symmetrical equivalence (Figure 5, Table 3S). The molecular packing of **3** is shown in Figure 6, where there are no intermolecular interactions between neighboring molecules of **3**.

Structure of $[Cu_4(\mu_3\text{-}O)_2(\mu\text{-admtrz})_4(admtrz)_2(\mu\text{-piv})_2(piv)_2]\cdot 2[Cu_2(\mu\text{-}H_2O)(\mu\text{-admtrz})(piv)_4]\cdot 13H_2O$ (4 = 4a·2(4b)·13H$_2$O). There are two kinds of molecules cocrystallized in **4**. The molecular structure of **4a** consists of a tetranuclear $[Cu_4(\mu_3\text{-}O)_2]$ core with a center of inversion [Figure 7a]. Both the Cu1---Cu2$^{\#1}$ edge and its symmetrical equivalence are spanned by admtrz ligands, while there are 1,3-bridging pivalate ligands at the other two edges. Cu2 is in a tetragonal pyramidal configuration ($\tau = 0.13$).[19] The four basal atoms are two triply bridging O atoms [Cu2−O1, 1.959(2) Å; Cu2−O1$^{\#1}$, 1.989(2) Å], N9 from one bridging admtrz ligand [Cu2−N9, 2.008(3) Å] and O2 from one bridging pivalate ligand [Cu2−O2, 2.007(2) Å]. The apical position is occupied by N2 from one bridging admtrz [Cu1−N2, 2.230(3) Å]. Cu1 exhibits a Jahn−Teller distorted octahedron configuration constructed with the triply bridging O atom [Cu1−O1, 1.979(2) Å], N5 from one terminal admtrz [Cu1−N5, 2.017(3) Å], N1$^{\#1}$ from one bridging admtrz [Cu1−N1$^{\#1}$, 2.041(3) Å], O4 from one terminal pivalate ligand [Cu1−O4, 2.015(3) Å], O3 from one 1,3-bridging pivalate ligand (Cu1−O3, 2.372(3) Å), and N10$^{\#1}$ from one bridging admtrz [Cu1−N10$^{\#1}$, 2.450(3) Å]. The Cu1---Cu2$^{\#1}$ edge distance of 3.2783(8) Å corresponding to two bridging admtrz ligands is shorter than that [3.4421(8) Å] of the Cu1---Cu2 edge corresponding to one bridging pivalate. The triply bridging O1 atom is 0.621 Å apart from the Cu_4 plane, and the three bond angles around O1 are 121.89(11)° (Cu1−O1−Cu2), 97.65(9)° (Cu2−O1−Cu2$^{\#1}$), and 111.42(10)° (Cu1−O1−Cu2$^{\#1}$), respectively. To the best of our knowledge, **4a** is the first example of tetranuclear Cu(II) complex with a $[Cu_4(\mu_3\text{-}O)_2]$ core, whereas a considerable number of Cu(II) complexes with a $[Cu_4(\mu_3\text{-}OH)_2]$[22] or $[Cu_4(\mu_3\text{-}OR)_2]$[23] core are known.

4b is a dinuclear Cu(II) compound bridged with one water and one admtrz [Figure 7b]. Each of two Cu(II) ions is surrounded by oxygen atoms from two terminal pivalate ligands, oxygen atom from one bridging water molecule, and nitrogen atom from one bridging admtrz. The distance of Cu3---Cu4 is 3.2740(9) Å. The deviations of Cu3 from the Cu3−O6−O9−O7−N13 plane (a) and Cu4 from the Cu4−O6−N14−O13−O11 plane (b) are −0.0492(14) and 0.0101(13) Å, respectively. The dihedral angle between (a) and (b) is 33.75(8)°. There are three types of intramolecular hydrogen bonds, O6−H6b···O11, O6−H6b···O12, and O6−H6a···O10, between bridging water and two terminal pivalate ligands [Figure 7b, Table 4S]. Although the water bridge spanning two Cu(II) ions has been observed in some Cu(II) complexes,[21a] **4b** is the first dinuclear water bridged Cu(II) complex with a derivative of 1,2,4-triazole.

As shown in Figure 8, one-dimensional chain structure is formed along the *b* axis through nine intermolecular hydrogen bonds, N4−H4D···O18$^{\#1}$, N4−H4E···O8, N4−H4E···O9, N8−H8E···O12$^{\#1}$, N12−H12E···O17$^{\#2}$, O17−H17D···O10, O17−H17E···O11, O18−H18A···O5$^{\#1}$, and O18−H18B···O17$^{\#2}$ (Table 4S).

EPR Studies. The X-band 110 K EPR spectra of **1**−**3** on polycrystalline samples and in frozen solutions are shown

(22) (a) Murugavel, R.; Sathiyendiran, M.; Pothiraja, R.; Walawalkar, M. G.; Mallah, T.; Riviére, E. *Inorg. Chem.* **2004**, *43*, 945−953. (b) Knuuttila, P. *Inorg. Chim. Acta* **1982**, *58*, 201−206. (c) Gou, S.; Qian, M.; Yu, Z.; Duan, C. Y.; Sun, X. F.; Huang, W. *J. Chem. Soc., Dalton Trans.* **2001**, 3232−3237. (d) Little, R. G.; Moreland, J. A.; Yawney, D. B. W.; Doedens, R. J. *J. Am. Chem. Soc.* **1974**, *96*, 3834−3842. (e) Dong, G.; Baker, A. T.; Craig, D. C. *Inorg. Chim. Acta* **1995**, *231*, 241−244. (f) Guerriero, P.; Ajo, D.; Vigato, P. A.; Casellato, U. *Inorg. Chim. Acta* **1988**, *141*, 103−118. (g) Chen, L.; Thompson, L. K.; Bridson, J. B. *Inorg. Chem.* **1993**, *32*, 2938−2943. (h) Mezei, G.; Rivera-Carrillo, M.; Raptis, R. G. *Inorg. Chim. Acta* **2004**, *357*, 3721−3732. (i) Sain, S.; Maji, T. K.; Mostafa, G.; Lu, T.-H.; Ribas, J.; Tercero, X.; Chaudhuri, N. R. *Polyhedron* **2003**, *22*, 625−631. (j) Mathews, I. I.; Manohar, H. *J. Chem. Soc., Dalton Trans.* **1991**, 2139−2143. (k) van Albada, G. A.; Mutikainen, I.; Roubeau, O.; Turpeinen, U.; Reedijk, J. *Inorg. Chim. Acta* **2002**, *331*, 208−215.

(23) (a) Tandon, S. S.; Thompson, L. K.; Bridson, J. N.; Bubenik, M. *Inorg. Chem.* **1993**, *32*, 4621−4631. (b) Masi, D.; Mealli, C.; Sabat, M.; Sabatini, A.; Vacca, A.; Zanobini, F. *Helv. Chim. Acta* **1984**, *67*, 1818−1826. (c) Breeze, S. R.; Wang, S.; Greedan, J. E.; Raju, N. P. *J. Chem. Soc., Dalton Trans.* **1998**, 2327−2333. (d) Koikawa, M.; Yamashita, H.; Tokii, T. *Inorg. Chim. Acta* **2004**, *357*, 2635−2642. (e) Tangoulis, V.; Raptopoulou, C. P.; Paschalidou, S.; Tsohos, A. E.; Bakalbassis, E. G.; Terzis, A.; Perlepes, S. P. *Inorg. Chem.* **1997**, *36*, 5270−5277.

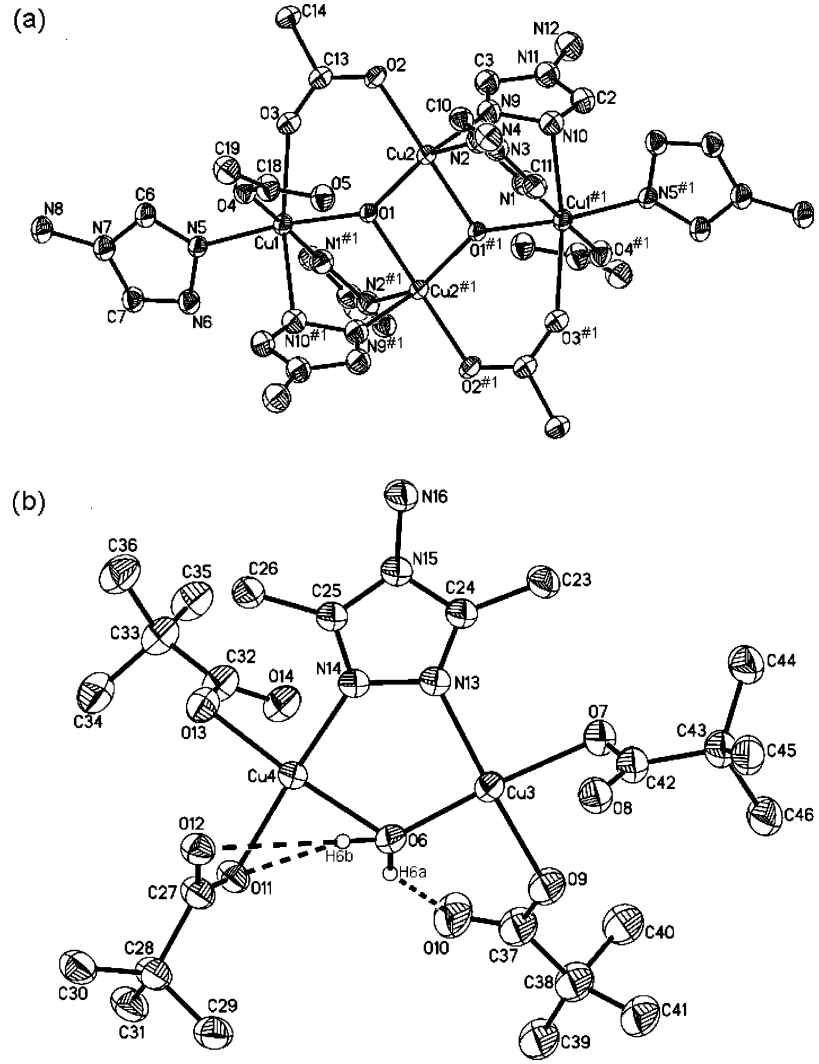

Figure 7. ORTEP drawing (30% probability level) of **4**. Top (a) **4a**; bottom (b) **4b**. All H atoms (except H6a and H6b), lattice water, methyl groups in pivalates and admetrz in (a) have been omitted for clarity [symmetry code: #1, $1 - x$, $1 - y$, $2 - z$].

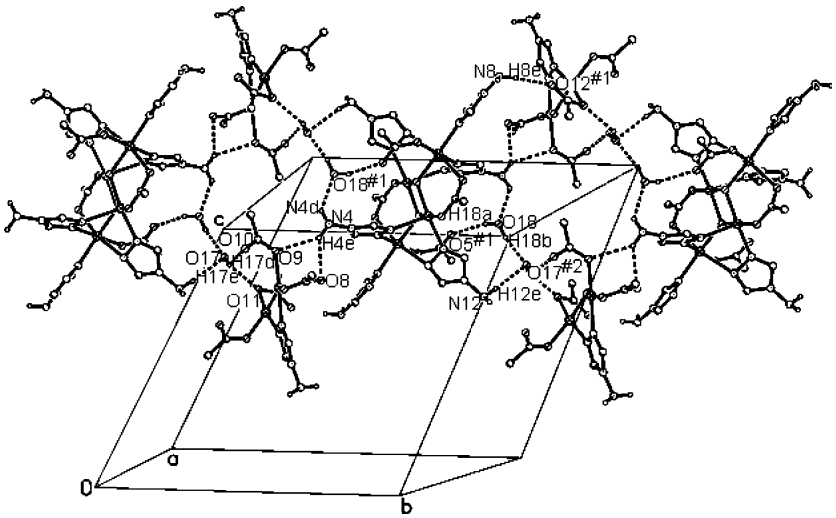

Figure 8. The molecular packing of **4**. Methyl groups in pivalates and admetrz have been omitted for clarity [symmetry code: #1, $-x + 1$, $-y + 1$, $-z + 2$; #2, x, $y + 1$, z].

in Figure 9. The EPR parameters for **1**−**3** derived from these EPR spectra are listed in Table 6. The powder EPR spectra of **1**−**3** measured at 110 K exhibit an axial spectrum showing signals at $g_{\parallel}$ and $g_{\perp}$ typical for a Cu^{II} ion with the $d(x^2-y^2)$ ground state (Figure 9a,c,e). Furthermore, an obvious superhyperfine splitting of the g component was observed in the

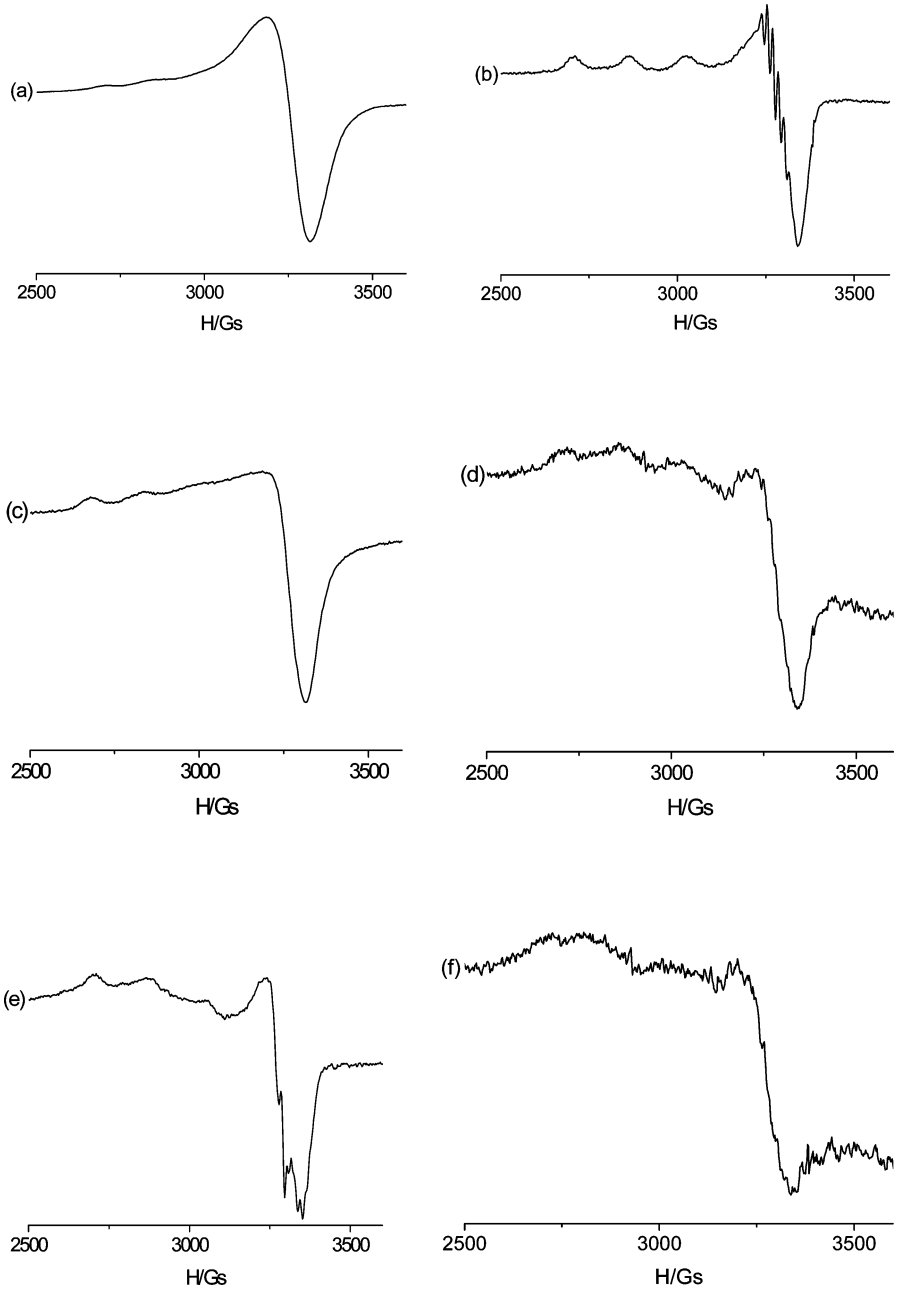

Figure 9. X-band EPR spectra of **1**−**3**: (a) powder **1** at 110 K (frequency 9.4856 GHz); (b) **1** in DMF at 110 K (frequency 9.4842 GHz); (c) powder **2** at 110 K (frequency 9.429 GHz); (d) **2** in MeOH at 110 K (frequency 9.4857 GHz); (e) powder **3** at 110 K (frequency 9.4843 GHz); and (f) **3** in EtOH at 110 K (frequency 9.4846 GHz).

Table 6. X-band EPR Parameters for **1**−**3**[a]

	$g_\perp$	$g_{\|\|}$	g_{av}	A_{Cu} (Gs)	A_N (Gs)
1(solid)	2.0449	2.3636	2.1511	141	
1(DMF)	2.0291	2.3307	2.1296	160	16
2(solid)	2.0313	2.3526	2.1384	155	
2(MeOH)	2.0295				
3(solid)	2.0399	2.3292	2.1363	167	14
3(EtOH)	2.0292				

[a] $g_{av} = (g_{\|\|} + 2g_\perp)/3$.

powder spectrum for **3** (Figure 9e), which is due to the electronuclear interaction from the adjacent ^{14}N atoms of the tbtrz ligand coordinated to the Cu(II) ions. In frozen DMF solution of **1**, signals at $g_{\|\|}$ and $g_\perp$ typical for a Cu^{II} ion with the d(x^2-y^2) ground state were observed, exhibiting a superhyperfine splitting. The EPR signals of **2** and **3** in frozen solution were relatively weak. As seen from Table 6, the EPR parameters derived from the frozen solution spectra are comparable to those obtained in powder samples, indicating that the coordinating geometries of Cu(II) ions and the structures of molecules in solid are probably retained in solution.

Magnetic Properties of 1−3. The magnetic susceptibility data for polycrystalline samples of **1**−**3** are displayed as plots of χ_m and $\chi_m T$ versus temperature (T) in Figures 10−12, respectively.

It has been experimentally demonstrated that the unpaired electron of the square-pyramidal Cu^{II} center is in a magnetic orbital of d(x^2-y^2) symmetry, which is situated in the basal plane of the coordination sphere around the Cu^{II} ion and is partially delocalized on the axial ligands. The unpaired

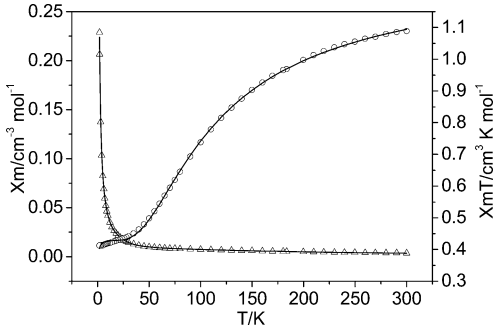

Figure 10. Plots of χ_m (△) and χ_mT (○) versus temperature for **1**, where the solid line represents the theoretical curve.

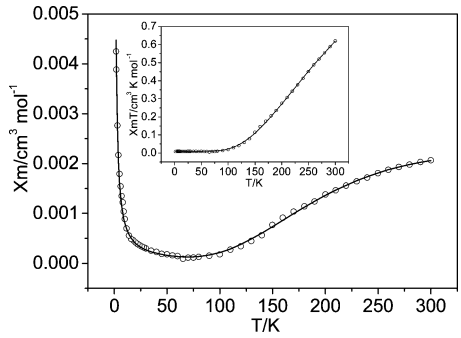

Figure 11. Plots of χ_m and χ_mT (inset) versus temperature for **2**, where the solid line represents the theoretical curve.

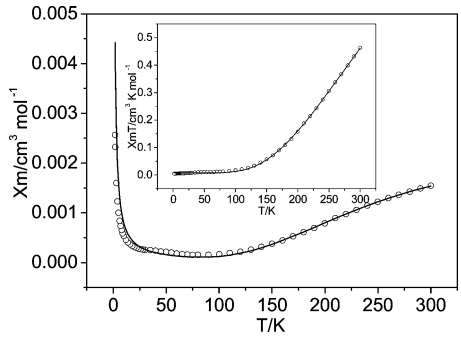

Figure 12. Plots of χ_m and χ_mT (inset) versus temperature for **3**, where the solid line represents the theoretical curve.

electron density along the d(z^2) orbital could be indicated by the Addison parameter (τ):[19] for $\tau = 0$ (the least) and for $\tau = 1$ (the largest). The magnetic orbitals located on the Cu^{II} ions are only favorably oriented to yield a considerable overlap on magnetic orbitals of bridging atoms to transfer magnetic interactions in many polynuclear Cu(II) complexes. Hatfield and Hodgson[24] proposed an empirical magneto-structural correlation: the Cu−OH−Cu pathway with a Cu−OH−Cu angle >97.6° mostly transfers antiferromagnetic interactions ($J < 0$), with an increasing antiferromagnetic interaction as the Cu−OH−Cu angle increases. This correlation is obeyed in the case of the symmetrical, planar systems with a pair of bridging hydroxide.[24] An empirical magnetostructural correlation has been found in triazole bridged dicopper compounds with a planar $Cu(N-N)_2Cu$ framework: a symmetric bridging model with the Cu−N−N angles close to 135° allows a stronger antiferromagnetic interaction than the less symmetric bridging model with a smaller Cu−N−N angle.[2] The above magnetostructural correlations could be used to rationalize the magnetic data of **1**−**3**, in which the magnetic interactions are mainly transferred by the bridging hydroxide and bridging *N*,*N*-triazole ligands.

(24) (a) Crawford, V. H.; Richardson, H. W.; Wasson, J. R.; Hodgson, D. J.; Hetefield, W. E. *Inorg. Chem*. **1976**, *15*, 2107−2110. (b) Ruiz, E.; Alemany, P.; Alvarez, S.; Cano, J. *Inorg. Chem.* **1997**, *36*, 3683−3688.

Scheme 2. Model for the Cu Cluster, with Bridging Oxygen (●) Joining Copper (○)[a]

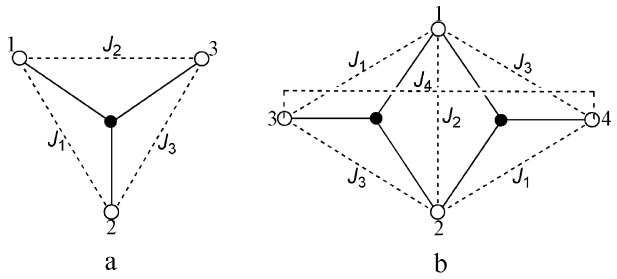

[a] The distinct exchange interactions are labeled.

The room-temperature value of χ_mT is 1.09 cm^3 K mol^{-1} for **1**, which is close to that expected for three uncoupled Cu^{II} ions with $g = 2.0$ (1.13 cm^3 K mol^{-1}). It decreases upon lowering the temperature to reach a value of 0.40 cm^3 K mol^{-1} at 1.8 K (one unpaired electron for $g = 2.065$). This magnetic behavior reveals that an overall antiferromagnetic interaction dominates the magnetic coupling and the ground state is $S = {}^1/_2$ (Figure 10). The molecular structure of **1** shows that three exchange parameters J_i are required to cover each possible pairwise exchange interaction between Cu^{II} ions (Scheme 2a), and thus the exchange Hamiltonian takes on the form in eq 1, in which exchange parameters J_1, J_2, and J_3 correspond to μ-adetrz/μ_3-hydroxide (e.g., Cu1···Cu2), μ-adetrz/μ_3-hydroxide (e.g., Cu1···Cu3), and μ_3-hydroxide (e.g., Cu2···Cu3) superexchange pathways, respectively.

$$\hat{H} = -2J_1(\hat{S}_1\hat{S}_2) - 2J_2(\hat{S}_1\hat{S}_3) - 2J_3(\hat{S}_2\hat{S}_3) \qquad (1)$$

The general analytical solution of eq 1[25] is used to fit the experimental data, and the intermolecular interactions are taken into account for the experimental variation of χ_mT at low temperature (eq 2).

$$\chi_m' = \chi_m/[1 - (2zJ/N\beta^2g^2)\chi_m] \qquad (2)$$

In the least-squares fit procedure, the g value of 2.151 derived from powder EPR spectrum is fixed. The best fitting gives −55.6, −28.5, −12.8 cm^{-1} for three values of exchange parameters J_i and $zJ = -0.21$ cm^{-1} with the agreement factor $R = 4.1 \times 10^{-5}$ ($R = \sum|(\chi_mT)_{exp} - (\chi_mT)_{calc})|^2/\sum(\chi_mT)_{exp}^2$). The problem of the assignment of three J values could be solved by relating the J values with the structural parameters. In **1**, the Cu3−N2−N1−Cu1 pathway involving the long axial bond distance of 2.260(3) Å (Cu1−N1) is expected not to have significant contributions to J_2, and thus J_2 is more negative than J_3 because the angle Cu3−O1−Cu1 [115.83(10)°] is larger than the angle Cu2−

(25) Kahn, O. *Molecular Magnetism*; VCH: New York, 1993.

O1−Cu3 [108.70(9)°]. The N6−N5−Cu1 [116.90(18)°] and N5−N6−Cu2 [115.59(17)°] angles deviate largely from 135°, which suggests the Cu1−N5−N6−Cu2 pathway transfers a weak antiferromagnetic interaction. Moreover, the Cu1−O1−Cu2 pathway has an effect similar to the Cu2−O1−Cu3 pathway due to their similar Cu−O−Cu angles [108.30(9)° vs 108.70(9)°]. Hence, J_1 should also be more negative than J_3. According to the above analyses, J_3 is assigned to the largest value of -12.8 cm^{-1}. However, it is rather difficult to assign J_1 and J_2, because there are insufficient examples to be ascribed to the effect of a particular structural factor. A weak exchange interaction of -17.7 cm^{-1} was found for the symmetrical triazole bridge pathway in the chainlike complex $[Cu(atrz)_2(N_3)]NO_3$.[6b] Thus, the Cu1−N5−N6−Cu2 pathway in **1** with the symmetrical bridging angles [116.90(18)°, 115.59(17)°] smaller than those (121.0°, 122.3°) of $[Cu(atrz)_2(N_3)]NO_3$ could be expected to give a larger J value than -17.7 cm^{-1}. In the end, J_1 and J_2 might be tentatively assigned to the values of -28.5 and -55.6 cm^{-1}, respectively.

The room-temperature value of $\chi_m T$ is 0.62 cm^3 K mol^{-1} for **2** and is significantly smaller than the value expected for four uncoupled Cu^{II} centers with $g = 2.0$ (1.5 cm^3 K mol^{-1}). This value of $\chi_m T$ drops quite rapidly with decreasing temperature to reach a practically diamagnetic behavior below 60 K. This magnetic behavior reveals that the spin magnetic moments of the Cu^{II} centers are strongly coupled antiferromagnetically and the ground state is $S = 0$ (Figure 11). The trend of the data in the χ_m versus T plot at the low-temperature range (∼20−1.8 K) indicates a small amount of a paramagnetic impurity exists. Four exchange parameters J_i are required to cover each possible pairwise exchange interaction between Cu^{II} ions (Scheme 2b). Thus, the exchange Hamiltonian takes on the form in eq 3, in which exchange parameters J_1, J_2, and J_3 correspond to μ-atrz/μ_3-hydroxide (e.g., Cu1···Cu2), double μ_3-hydroxide (e.g., Cu2···Cu2$^{\#1}$), and single oxygen bridge of piv/μ-piv/μ_3-hydroxide (e.g., Cu1···Cu2$^{\#1}$) superexchange pathways, respectively, and J_4 is assumed to be zero due to the large Cu1---Cu1$^{\#1}$ distance [5.712(1) Å].

$$H = -2J_1(\hat{S}_1\cdot\hat{S}_3 + \hat{S}_2\cdot\hat{S}_4) - 2J_2\hat{S}_1\cdot\hat{S}_2 - 2J_3(\hat{S}_1\cdot\hat{S}_4 + \hat{S}_2\cdot\hat{S}_3) - 2J_4\hat{S}_3\cdot\hat{S}_4 \quad (3)$$

The general analytical solution of eq 3[26] is used to fit the experimental data, and a correction ρ is introduced to take into account the percentage of paramagnetic impurities ($S = {}^1/_2$). In the fit procedure, the g value of 2.138 derived from powder EPR spectra is fixed. The least-squares fitting leads to the following parameters: $J_1 = -216.5$, $J_2 = -17.2$, $J_3 = -15.7$ cm^{-1}, and $\rho = 0.47\%$ with $R = 1.3 \times 10^{-4}$. These parameters obtained seem reasonable with a small value of R. However, there is specific point that must be addressed about the J_2 value. In **2**, the unpaired electron density along the d(z^2) orbital of Cu2 is expected to be very small ($\tau = 0.069$). The distance Cu2−O1$^{\#1}$ is 2.362(4) Å. Thus, the poor overlap between the magnetic orbitals centered on Cu2 and Cu2$^{\#1}$ suggests that the interactions involving the axially long bond pathway are estimated to be negligible.[27] A very weak magnetic coupling of 0.34 cm^{-1} was found for the axially long bond pathway in the "stepped wise" complex $[Cu_4(\mu_3\text{-}OH)_2(\mu\text{-}OH)_2(2,2'\text{-bipy})_4Cl_2]Cl_2\cdot 6H_2O$.[22i] Furthermore, the angle Cu2−O1−Cu2$^{\#1}$ (95.21(14)°) implies a positive value for J_2. A rational fitting is accomplished with a fixed $J_2 = 0$, leading to parameters: $J_1 = -216.4$, $J_3 = -21.0$ cm^{-1}, and $\rho = 0.47\%$ with $R = 1.3 \times 10^{-4}$.

The $\chi_m T$ versus T plot of **3** is very similar to that of **2** (Figure 12). The room-temperature $\chi_m T$ value of 0.46 cm^3 K mol^{-1} is smaller than that of **2** (0.62 cm^3 K mol^{-1}), which indicates stronger antiferromagnetic interactions between the Cu^{II} centers than those in **2**. The ground state is $S = 0$. The spin Hamiltonian used to describe the isotropic exchange interactions is the same as that of **2**, as expected by their similar structures. In the least-squares fit procedure, the g value of 2.136 derived from the powder EPR spectrum is fixed. The best fitting result is $J_1 = -270.2$, $J_2 = 173.3$, $J_3 = 2.3$ cm^{-1}, and $\rho = 0.47\%$ with $R = 2.6 \times 10^{-4}$, in which the unusual large positive value of J_2 is physically pointless according to the same analysis as the J_2 in **2**. The rational fitting with the fixed $J_2 = 0$ leads to the parameters: $J_1 = -259.8$, $J_3 = 4.8$ cm^{-1}, and $\rho = 0.48\%$ with $R = 3.0 \times 10^{-4}$.

Strong antiferromagnetic coupling in **2** ($J_1 = -216.4$ cm^{-1}) and **3** ($J_1 = -259.8$ cm^{-1}) is mainly due to the Cu−OH−Cu pathway in the equatorial plane [Cu2−O1−Cu1, 123.72(18)° in **2**; Cu2$^{\#1}$−O1−Cu1, 123.33(13)° in **3**]. The Cu−N−N−Cu pathway might give a limited contribution, because the correlative N−N−Cu angles [125.0(4)°, 119.1(3)° in **2**, 120.6(3)°, 119.7(2)° in **3**] are smaller than the most optimized bridging angle of 135°.

Conclusions

The syntheses, structures, and magnetic properties of four polynuclear copper(II) complexes with derivatives of 1,2,4-trizole and pivalate ligands have been presented. The successful isolation of **1**−**4** confirms that the mixed, versatile pivalate and the derivatives of 1,2,4-triazole ligands are effective in forming the nonlinear polynuclear metal complexes. The magnetic susceptibility data show that antiferromagnetic exchanges dominate in **1**−**3**, as expected from their structures.

Acknowledgment. We thank the reviewers for their helpful comments. This work was supported by the Distinguished Overseas Young Fund from the Natural Science Foundation of China (No. 20028101), the Program for Changjiang Scholars and Innovative Research Team in University, the Natural Science Grant of Jiangsu Province (BK 2004087), the Nature Science Foundation of China

(26) Song, Y.; Massera, C.; Roubeau, O.; Gamez, P.; Lanfredi, A. M. M.; Reedijk, J. *Inorg. Chem.* **2004**, *43*, 6842−6842.

(27) Aromí, G.; Ribas, J.; Gamez, P.; Roubeau, O.; Kooijman, H.; Spek, A. L.; Teat, S.; MacLean, E.; Stoeckli-Evans, H.; Reedijk, J. *Chem.-Eur. J.* **2004**, *10*, 6476−6488.

(20001004), the Foundation of Instruments of Nanjing University, and the U.S. National Science Foundation.

Supporting Information Available: X-ray crystallographic files in CIF format and tables for the hydrogen bonding for **1**−**4** (Tables 1S−4S). This material is available free of charge via the Internet at http://pubs.acs.org. Crystallographic data of **1**−**4** have been deposited with the Cambridge Crystallographic Data Centre as a supplementary publication. Deposition codes: 249506 for **1** and 265571 for **2**, 265570 for **3** and 266934 for **4**. Copies of the data can be obtained free of charge on application to CCDC, 12 Union Road, Cambridge CB2 1EZ, UK [Fax: (+44)1223-336-033. E-mail: deposit@ccdc.cam.ac.uk].

IC050475X